Solar Phys (2010) 267: 329–342
DOI 10.1007/s11207-010-9642-0

Types of Microwave Quasi-Periodic Pulsations in Single Flaring Loops

E.G. Kupriyanova · V.F. Melnikov · V.M. Nakariakov · K. Shibasaki

Received: 12 October 2009 / Accepted: 19 September 2010 / Published online: 2 November 2010

Abstract Quasi-periodic pulsations (QPP) of microwave emission generated in single flaring loops observed with the *Nobeyama Radioheliograph* (NoRH) and *Nobeyama Radio Polarimeters* (NoRP) are studied. Specific features of the time profiles, *i.e.* the visible presence or absence of QPPs, are not accounted for in the selection. The time evolution of the periods of the QPPs is examined using wavelet and correlation analyses. In ten out of twelve considered events, at least one or more significant spectral components with periods from 5 – 60 s have been found. The quality of the oscillations is rather low: $Q = \pi N$, where N is the number of cycles, mostly varies in the range 12 to 40, with an average of 25. We suggest that the detected QPPs can be classified into four types: *i*) those with stable mean periods (*e.g.* of 15 – 20 s or 8 – 9 s, the prevailing type); *ii*) those with spectral drift to shorter periods (mostly in the rise phase of the microwave emission); *iii*) those with drift to longer periods (mostly in the decay phase); *iv*) those with multiple periods showing an X-shaped drift (*e.g.* in the range from 20 – 40 s in the rise phase).

Keywords Flares, impulsive phase · Oscillations, solar · Radio bursts, microwave

1. Introduction

Quasi-periodic pulsations (QPPs) are a common feature of the flare energy release process. The periods of QPPs can be split into several bands, from sub-seconds up to tens of minutes. "Short" (sub-second) QPPs in the m-dm-cm radio emission are likely to be associated

E.G. Kupriyanova (✉) · V.F. Melnikov
Central Astronomical Observatory at Pulkovo of the Russian Academy of Sciences,
Saint-Petersburg 196140, Russia
e-mail: elenku@bk.ru

V.F. Melnikov · K. Shibasaki
Nobeyama Solar Radio Observatory, Minamimaki, Minamisaku, Nagano 384-1305, Japan

V.M. Nakariakov
Physics Department, University of Warwick, Coventry, UK

with kinetic processes caused by the dynamic interaction of electromagnetic, plasma or whistler waves with energetic particles trapped in closed magnetic fields during solar radio bursts (see, *e.g.* Aschwanden, 1987; Fleishman *et al.*, 2002). "Long" QPPs, with periods from several to tens of minutes, are usually associated with active region dynamics and global oscillations of the Sun (Gelfreikh *et al.*, 1999; Shibasaki, 2001; O'Shea *et al.*, 2001; McAteer *et al.*, 2004; Gelfreikh, Nagovitsyn, and Nagovitsyna, 2006). "Medium period" (seconds to several minutes) QPPs detected in microwave, white light, EUV and X-ray emissions are likely to be associated with magnetohydrodynamic (MHD) processes in solar flaring loops. Recently, they have attracted strong attention because of the newly opened possibility of observing such QPPs directly using instruments with high spatial resolution. In particular, the *Nobeyama Radioheliograph* (NoRH) has sufficiently high angular ($5''$ and $10''$ at 34 GHz and 17 GHz, respectively) and temporal (100 ms) resolutions, allowing the determination of the spatial structure of the pulsating regions, their phase relations and the fine temporal and spectral structure of the QPPs. Also, medium QPPs are interesting due to their possible association with the fundamental physical processes operating in flares: spontaneous and triggered energy releases, magnetic reconnection, thermodynamics, MHD oscillations, particle acceleration and other kinetic effects (see Nakariakov and Melnikov, 2009 for a review). In this paper, we concentrate our attention on the "medium" QPPs only.

Asai *et al.* (2001) obtained the first imaging microwave observations of flaring QPPs in the event of 10 November 1998 using NoRH. A detailed analysis of this event by Grechnev, White, and Kundu (2003) suggested an interpretation in terms of propagating fast magnetoacoustic or torsional waves.

The first attempt to utilise spatial information for the interpretation of QPPs in a simple single flaring loop was undertaken by Nakariakov, Melnikov, and Reznikova (2003), Melnikov *et al.* (2005), and Reznikova *et al.* (2007), for the flare on 12 January 2000. The event was found to have two well-defined periods of about 16 s and 10 s. Using the observed length and width of the flaring loop as well as results of microwave diagnostics of the plasma density and magnetic field strength, the authors have demonstrated that the observed oscillations were produced by two magnetoacoustic standing modes. The longer period oscillation was shown to be produced by the global sausage mode. The presence of multiple periodicities in QPPs opens up interesting perspectives for plasma diagnostics (see, *e.g.* Andries *et al.*, 2009 and references therein). Also, Inglis and Nakariakov (2009) have shown that for the flares exhibiting QPPs with several significant periods, the determination of the mechanism for the generation of QPPs can be based on the comparative analysis of the period ratios.

Foullon *et al.* (2005) found an instructive example of QPPs with similar periods of several minutes, occurring at two spatially separated active regions on 5 – 6 February 2003, and demonstrated that the periodic energy releases could be triggered by kink oscillations of a long EUV transequatorial loop linking those regions. The triggering mechanism can be connected with the periodic generation of anomalous resistivity in the vicinity of coronal magnetic null points, causing fast magnetic reconnection, by the magnetoacoustic oscillation in the external loop (Nakariakov *et al.*, 2006). Very recently, Zimovets and Struminsky (2009) analysed QPPs with periods of a few minutes in the two-ribbon flares of 29 May 2003 and 19 January 2005. The QPPs were interpreted in terms of the external triggering mechanism; however, other options were not excluded. The occurrence of similar (in period, quality and modulation depth) QPPs in both single-loop and two-ribbon flare scenarios may indicate the common origin of the periodicity.

A different approach was implemented by Fleishman, Bastian, and Gary (2008) in the analysis of the limb flare on 15 June 2003, which was simultaneously observed by NoRH, the *Owens Valley Solar Array* and the *Nobeyama Radio Polarimeters* (NoRP). The observed

properties of the QPPs were compared with those derived from two simple models for the radio emission, one considering MHD oscillations in the emitting plasma and the other the quasi-periodic injection of fast electrons. Fleishman, Bastian, and Gary (2008) concluded that the observations were consistent with quasi-periodic particle injection (without its specification). We would like to point out that magnetic reconnection, externally triggered by an MHD oscillation, also fits the observables.

The above-mentioned medium QPPs usually last for three to seven cycles, so their quality is rather low: $Q = \pi N \approx 10-20$ (where N is the number of cycles). In addition, full Sun observations have revealed another type of medium QPP that is characterised by very high quality ($Q > 100$). Such long-lasting high quality oscillations were detected with a large single dish antenna at the Metsahovi Radio Observatory at 22 and 37 GHz (see Zaitsev and Stepanov, 2008 for a review). The oscillations have periods in the range $0.5-10$ s and positive or negative frequency drifts. Sometimes, two spectral components of different periods were observed simultaneously, having opposite frequency drifts. The spectral branches were seen to intersect with each other (an X-type intersection). Zaitsev *et al.* (1998) and Khodachenko *et al.* (2009) interpreted these oscillations in terms of the LCR-circuit model. Detailed studies of these types of pulsations using observations with high spatial resolution are needed.

Until now, high spatial resolution microwave observations have been used in the analysis of several QPP events only. All of the events were selected based on the visible presence of well-indicated QPP patterns in the light curves. Evidently, there is a strong need for a more general study. The purpose of this paper is to carry out a statistically broader study based upon the analysis of twelve well-resolved "single flaring loops", seeking answers to the following questions: *i*) Is the presence of QPPs in flaring loops a common phenomenon? *ii*) How often may more than one spectral component occur in a single flaring loop, and is multi-periodicity a common feature of QPPs? *iii*) What is the characteristic evolution of the QPP spectrum during the flare? These questions are important for the understanding of the physical mechanism, or group of mechanisms, responsible for the generation of QPPs in solar and stellar flares.

The paper is organised as follows. In Section 2 we discuss the data used in this study, data reduction techniques and the rules applied to the selection of the analysed events. Section 3 describes the data analysis and its results, and the four types of QPPs which are identified in this paper. The possible implications of the results are discussed in Section 4.

2. Observations and Data Reduction

Our selection criteria for the analysis of flaring sources are as follows. The microwave source should: *i*) be well resolved by NoRH, that is, its length should be larger than the beam size at 17 GHz; *ii*) have a single loop shape; *iii*) be located near the solar disk centre, or have relatively small intensity if located near the limb, reducing the influence of positional ambiguity in the image synthesis. Specific features of the radio emission time profiles, *i.e.* the visible presence or absence of QPPs, are not accounted for in the selection. In other words, events without a pronounced QPP pattern are not excluded from our consideration. As a result, we have chosen 12 single flaring loops observed in the period 2002 – 2005. The image of one of them, typical for the analysed class of flares, is shown in Figure 1.

Table 1 lists the selected flares and their characteristics (heliographic coordinates, GOES class, loop size, duration of the impulsive phase, peak flux at 17 GHz). The information is taken from the Nobeyama Radio Observatory official internet site (http://solar.nro.nao.ac.jp/).

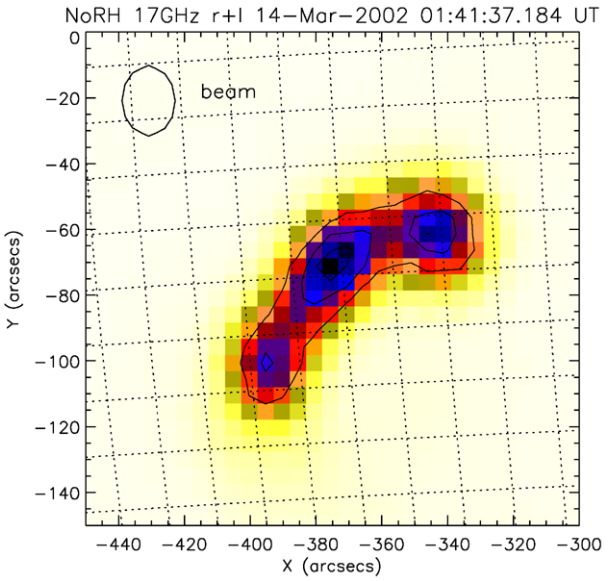

Figure 1 The flaring loop observed by the *Nobeyama Radioheliograph* at 17 GHz at the beginning of the event on 14 March 2002. The pixel size is $4.91''$. Contours show levels 0.50, 0.75 and 0.90 of the maximum brightness. The beam half-width is shown in the upper left corner.

Table 1 Observed characteristics of the selected events.

Burst date and time of maximum	Helio coordinates	X-ray class	Loop length, 10^7 m	Duration at 17 GHz (impulsive phase)	Peak flux at 17 GHz, sfu
14 Mar 2002 01:43:46 UT	S10E23	M5.7	6.6	16 m	799
31 May 2002 00:07:25 UT	S30E85	M2.4	2.5	9 m	180
03 Jul 2002 02:10:10 UT	S19W48	X1.5	2.5	7 m	768
18 Jul 2002 03:32:53 UT	N19W27	M2.2	3.1	5 m 20 s	1984
28 Jul 2002 23:01:28 UT	S12W07	M2.2	4.7	4 m	486
12 Aug 2002 02:17:23 UT	S06E78	C1.4	2.5	2 m	276
18 Aug 2002 22:47:22 UT	S07W22	–	4.9	4 m	205
17 Mar 2003 00:59:59 UT	S15W26	C3.1	3.1	15 m	224
27 Oct 2003 01:35:31 UT	S20E29	C6.2	4.5	2 m 40 s	1515
21 May 2004 23:50:14 UT	S10E53	–	2.5	14 m	342
22 Jul 2004 00:31:15 UT	N05E16	M9.1	7.4	1 h 20 m	362
22 Aug 2005 00:54:59 UT	S12W49	M2.6	3.9	1 h 05 m	382

The loop size is determined from the flare radio brightness distribution at 34 GHz, where NoRH has better resolution. The loop lengths are measured at the moment when all their parts have already developed. Distances d between centres of the flaring loop footpoints have been transformed into linear loop size, assuming that the loop has a semicircular shape with a radius of $d/2$. The errors in determining the loop lengths are about $\pm 0.2 \times 10^7$ m, which corresponds to half of the NoRH beam size at 34 GHz. The duration of the impulsive phase is taken at the level of 0.1 of the peak flux at 17 GHz. The peak flux at 17 GHz is shown in solar flux units (1 sfu $= 10^{-22}$ W m^{-2} Hz^{-1}).

The evolution of the selected events is analysed with two independent instruments, NoRP and NoRH. This gives us the opportunity to exclude spectral components of instrumental origin. The NoRP radio telescopes receive integrated emission from the whole Sun at frequencies 1, 2, 3.75, 9.4, 17, and 35 GHz. For this study we have used the total flux density at $f = 17$ GHz and $f = 35$ GHz, received by NoRP, and the mean correlation amplitude records at $f = 17$ GHz and $f = 34$ GHz, obtained with NoRH. The mean correlation amplitude is calculated by averaging the amplitudes of the observed correlation coefficients between signals received by pairs of remote single antennas (separated by distances larger than $100L_{\min}$, where $L_{\min} = 1.528$ m is the minimum antenna spacing). The mean correlation amplitude represents an integrated radio flux, similar to that of NoRP. However, it measures integrated radio fluxes only from fine spatial structures (compact flaring sources) smaller than about $24''$. [1] The advantages of interferometric NoRH observations, in comparison with the integration of the radio signal over the whole Sun, are much better sensitivity and the efficient elimination of background emission from the Sun, the Earth's atmosphere and other objects.

There is an extensive literature on methods of detection of QPPs and identification of oscillatory components of solar emissions (see O'Shea *et al.*, 2001; McAteer *et al.*, 2004; Dmitriev *et al.*, 2006; Reznikova *et al.*, 2007, and references therein). In the current study we use several of them. Our procedure for a spectral analysis of signals is as follows. The flux density time profiles of the events, $F_{\rm f}(t)$, are smoothed over an interval τ that is usually greater than the expected period of the QPP. This gives us the slowly varying component $F_{\rm f}^{\rm sm}(t)$. The high frequency component is obtained by subtraction of the slowly varying component from the original time series,

$$F_{\rm f}^{\rm hf}(t) = F_{\rm f}(t) - F_{\rm f}^{\rm sm}(t). \tag{1}$$

Then, we obtain the modulation signal,

$$\Delta_{\rm f}(t) = F_{\rm f}^{\rm hf}(t)/F_{\rm f}^{\rm sm}(t). \tag{2}$$

This was done for a broad range of smoothing intervals: $\tau = 5$, 7, 10, 13, 15, 20, 25, 30, 40 s, allowing us to understand whether the spectral peak found is real or produced by the smoothing (filtering) procedure.

The suitability of this method for determining the reliability of the spectral components was verified by numerical simulations. For this we used the model function

$$f_1(t_{\rm i}) = f_{\rm b}(t_{\rm i})\big[1 + f_{\rm s}(t_{\rm i})\big] + f_{\rm n}(t_{\rm i}), \tag{3}$$

[1] See a detailed explanation in Nobeyama Radiohelograph Catalog of Events: 2003, *Nobeyama Radio Observatory* **4**, 3.

where t_i is the time of the measurement in seconds, $t_i = i$, where $i = 1, 2, 3, \ldots, N$ s; $f_b(t_i) = \sin(2\pi t_i/P_b)$ is a function defining the slowly varying background, with period $P_b = 3N$; $f_s(t_i) = \sum_{j=0}^{m} \tilde{A}_{sj} \sin(2\pi t_i/\tilde{P}_j)$ is a periodic component (signal) defined as the sum of m harmonic functions with different periods $\tilde{P}_j$ and amplitudes $\tilde{A}_{sj}$, $j = 0, \ldots, m$. The noise component $f_n(t_i)$ is defined as a numerical series of normally distributed random values with a mean value of zero and a standard deviation A_n which is either equal to the signal amplitude ($A_s/A_n = 1$) or twice larger than it ($A_s/A_n = 0.5$).

Our data analysis method was tested for different signal and noise functions given by Equation (3). We varied the number of periodic components, and their periods, amplitudes and signal-to-noise ratio. For each fixed set of these parameters, a noise function was tried 100 times in order to calculate deviations of values of a period estimated by our method from that obtained by Equation (3). We have found that despite the appearance of some spectral peaks caused by the noise function $f_n(t_i)$, the periodic component $f_s(t_i)$ is well distinguished in all cases. Moreover, errors in the period estimations are relatively small. For example, a signal with a given period and amplitude, *e.g.* $\tilde{P} = 16$ s and $\tilde{A}_s = 0.1$, is distinguished even in a short time series with $N = 100$. The scattering of period estimations, P_α, for different τ ($\tau = 5$, 7, 10, 13, 15, 20, 25, 30, 40 s) in the case of signal-to-noise ratio $A_s/A_n = 0.5$ is $|P_\alpha - \tilde{P}| \leq 2$ s and the mean period, $\bar{P}$, $|\bar{P} - \tilde{P}| \leq 1$ s in more than 90% of the cases. A decrease in the noise amplitude by a factor of two ($A_s/A_n = 1$) decreases the scattering, $|P_\alpha - \tilde{P}| \leq 1$ s and $|\bar{P} - \tilde{P}| \leq 1$ s, in more than 96% of the cases. An increase in the length of the time series up to $N = 300$ considerably increases the amplitude of the spectral peak of a periodogram and decreases its width at half power, as well as errors in the estimation of the period.

For the preliminary spectral analysis the time profiles $\Delta_f(t)$ were studied using wavelet (Morlet) analysis, in particular, the routines developed by Torrence and Compo (1998). Wavelet spectra give us the general spectral – time evolution of the analysed signal, and allow us to identify the candidate spectral – time intervals which may contain QPPs. Then, the candidate intervals are studied using auto-correlation, cross-correlation and Fourier methods, with the aim of determining the characteristic periods and their evolution, and the duration of phase conservation in the oscillations.

For the final analysis and classification, we have chosen only those oscillatory patterns which satisfy the following criteria. First, the oscillations should be well pronounced in the data from both instruments (NoRH and NoRP) and have similar frequency-time behaviour of the wavelet spectra. Second, they should be seen in periodograms of auto-correlation and cross-correlation functions at 17 and 34 GHz. Third, the value of their period should not depend upon the selected low frequency filter (the specific value of τ), at least inside the corresponding error bar. Fourth, their quality $Q = \pi N$ should exceed nine (that is, the number N of observed periods should be at least three).

3. Results of Data Analysis

In ten out of the twelve events under study, at least one significant oscillation with a period in the range from 5 – 60 s has been found (Table 2). The quality of the oscillations is rather low; it mostly varies in the range 12 to 40, with an average of 25, in only one case the quality reaches 85. Two oscillations were detected in two events, and one event was found to have three pronounced oscillations. In only two events significant periodicities, which would satisfy the imposed selection rules, were not found.

Table 2 List of detected periodicities.

Event	No.	Period, s	Frequency drift	Quality	Burst phase
14 Mar 2002	1	12.5	no	40	rise to maximum
	2	27 down to 9	yes	25	rise to maximum
31 May 2002	1	16 down to 9	yes	15	rise to maximum
03 Jul 2002	1	15	no	12	decay of the first peak
	2	20 up to 30	yes	15	decay of the burst
18 Jul 2002	1	9	no	12	rise – maximum
	2	17	no	12	whole flare
28 Jul 2002	1	8.5	no	35	whole flare
12 Aug 2002	1	12.5	no	12	rise
18 Aug 2002			no reliable spectral components		
17 Mar 2003	1	5	no	85	whole flare
	2	9	no	41	whole flare
	3	13	no	35	whole flare
27 Oct 2003	1	11.5	no	12	rise
21 May 2004	1	26 up to 38	yes	20	rise
	2	38 down to 26	yes	20	rise
	3	40 up to 60	yes	12	decay
22 Jul 2004	1	19	no	20	rise
	2	27	no	15	rise
22 Aug 2005			no reliable spectral components		

The properties of the QPPs found in this study are rather different. According to the time evolution, we divide the QPPs into four types: *i*) those with stable mean periods in the range 5 – 20 s (eight events); *ii*) those with spectral drift to shorter periods in the rise phase of the burst (two events); *iii*) those with drift to longer periods in the decay phase (two events); *iv*) those with an X-shaped drift between periods of 20 – 40 s (one event). We point out that the division into four types may be incomplete, and a larger number of events may reveal more characteristic types of pulsations.

The events illustrating each of these types are described in the following sub-sections and are shown in Figures 2 – 6. For each event, the colour panel demonstrates the wavelet power spectrum of the modulation signal $\Delta_f(t)$ for the NoRH data at 17 GHz. Six colours correspond to six power levels ranging from zero to the maximum value. Thin solid contours show 95% significance level, estimated according to Torrence and Compo (1998). For better visualisation, the normalised time profile of the radio emission intensity $F_f(t)$ is superimposed onto the wavelet spectrum by the thick solid line. Cross-hatched regions on either end of the wavelet spectra indicate the cone of influence. The small panel on the right of the wavelet spectrum represents the global wavelet power spectrum of the modulation signal. The dashed line on this plot defines the 95% significance level.

Each figure also shows the auto-correlation function of the modulation signal $\Delta_f(t)$ at 17 GHz and a set of periodograms (in units of spectral power normalised to the total variance), which correspond to different smoothing intervals τ. The dashed line in the panel with periodogram plots shows the 99% significance level estimated according to Horne and Baliunas (1986).

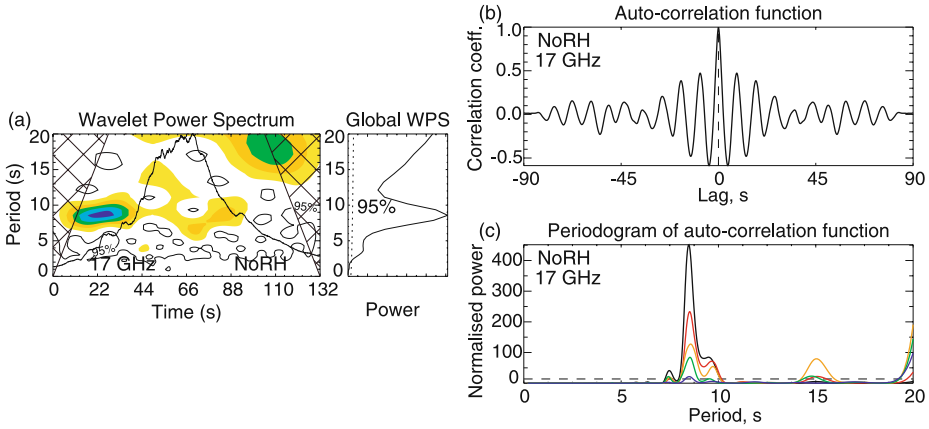

Figure 2 Wavelet and autocorrelation analyses of the flare on 28 July 2002, 23:00:20 – 23:02:32 UT, recorded with NoRH at 17 GHz. (a) Wavelet power spectrum of the modulation amplitude $\Delta_f(t)$, $\tau = 10$ s, with the superimposed normalised time profile $F_f(t)$ of the radio emission, both obtained with NoRH at 17 GHz. Thin solid contours show 95% significance level. The right plot is the global wavelet power spectrum of $\Delta_f(t)$. Dashed line shows the 95% significance level. (b) Auto-correlation function of the modulation amplitude $\Delta_f(t)$, $\tau = 10$ s. (c) Periodograms (in units of spectral power normalised to the total variance), of an auto-correlation function: black solid line for $\tau = 10$ s, red for $\tau = 15$ s, orange for $\tau = 20$ s, green for $\tau = 25$ s, blue for $\tau = 30$ s. The spectral power for $\tau = 20$, 25 and 30 s is multiplied by four to see details. The black colour periodogram corresponds to the auto-correlation function displayed in the upper panel. Black dashed line corresponds to the 99% significance level.

3.1. Pulsations with a Stable Mean Period

In our analysis we consider a QPP as having a stable mean period P if the drift rate is $dP/dt < 3$ s m^{-1}. Figure 2 shows a typical example of a QPP of the first type. A single spectral component with a stable period $P \approx 8-9$ s dominates in the wavelet power spectrum, especially during the rise phase of the flare (Figure 2a). The QPPs become fainter during the maximum phase of the flare and regain the strength in the decay phase of the flare, while not reaching the power level they have in the rise phase. The period of the pulsations stays stable over 100 s, reaching a quality $Q \approx 35$. The auto-correlation function of the QPP (Figure 2b) has a very pronounced oscillatory pattern over the time interval that includes several cycles. Hence, the pulsations keep the phase during a sufficiently long time. The periodogram of the auto-correlation function has an obvious peak at 8 – 9 s, which is consistent with the wavelet analysis. Reliability of the spectral peak is proved by coincidence of its position for periodograms taken for different smoothing times: $\tau = 10$ s (black line), 15 s (red line), 20 s (orange line), 25 s (green line), and 30 s (blue line).

An interesting case when two spectral components are present in the spectrum has been found in the flare on 18 July 2002, shown in Figure 3. Pulsations with two stable periods ($P_1 \approx 9.5$ s and $P_2 \approx 16.5$ s) are seen in both the wavelet spectrum (Figure 3a) and in the periodogram of the auto-correlation function (Figure 3c). For about 23 s (the elapsed time interval is 22 – 45 s) these periodicities are observed simultaneously (Figure 3a).

Altogether, eight events with pulsations of this type were found in our study (see Table 2). Two and three stable periodicities were found to occur simultaneously in the flares on 18 July 2002 and 18 March 2003, respectively. In the flare on 22 July 2004, two different non-overlapping periodicities occur in the rise phase. Thus, QPPs in those flares are of the same

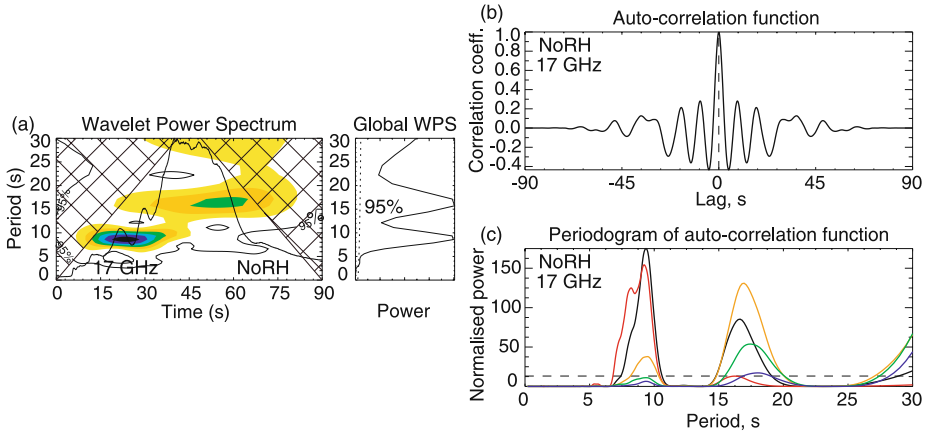

Figure 3 The same as Figure 2, but for the flare on 18 July 2002, 03:32:13 – 03:33:43 UT. Periodograms: black solid line for $\tau = 15$ s, red for $\tau = 10$ s, orange for $\tau = 20$ s, green for $\tau = 25$ s, blue for $\tau = 30$ s. The black colour periodogram corresponds to the auto-correlation function displayed in the upper panel.

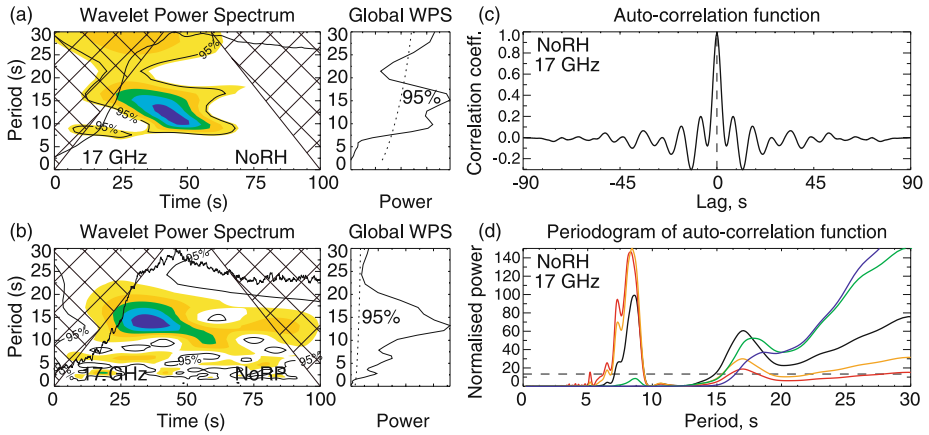

Figure 4 Analysis of the flare on 31 May 2002, 00:06:40 – 00:08:20 UT observed at 17 GHz. (a) Wavelet power spectrum of the modulation signal obtained for $\tau = 10$ s, with superimposed normalised profile of the radio emission, both obtained with NoRH. The right plot is the global wavelet power spectrum. The dashed line shows the 95% significance level. (b) The same as in panel (a) but for the NoRP data. (c) Auto-correlation function of the NoRH modulation signal. (d) Periodograms of the auto-correlation function: black solid line for $\tau = 10$ s, red for $\tau = 5$ s, orange for $\tau = 7$ s, green for $\tau = 15$ s, blue for $\tau = 20$ s. The black colour periodogram corresponds to the auto-correlation function displayed in the upper panel. Dashed line shows the 99% significance level.

type as in the event studied by Inglis and Nakariakov (2009), where three simultaneous significant periodicities were detected.

3.2. Pulsation with Spectral Drift to Shorter Periods

The flare on 31 May 2002 illustrates the second type of pulsations (Figure 4). Figure 4a and Figure 4b show the wavelet spectra of the modulation signals obtained with NoRH and

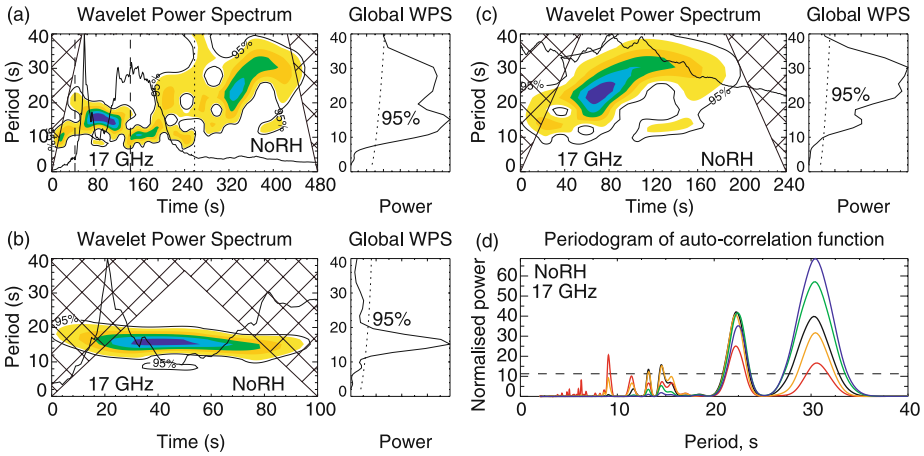

Figure 5 Analysis of the flare on 03 July 2002, 02:09:12 – 02:17:12 UT observed at 17 GHz. (a) Wavelet power spectrum of the modulation signal ($\tau = 15$ s) with superimposed normalised profile of the radio emission, both obtained with NoRH. Time interval between two vertical dashed lines indicates the occurrence of the first QPP. The time interval between the vertical dotted line to the end of the event indicates the occurrence of the second QPP. The right plot is the global wavelet power spectrum. The dashed line shows the 95% significance level. (b) Zoomed wavelet spectrum of the first QPP, from 02:09:50 to 02:11:30 UT. (c) Zoomed wavelet spectrum of the second QPP, from 02:13:30 to 02:17:30 UT. (d) Periodograms of the auto-correlation functions constructed for the modulation signal of the second QPP. Black solid line is for $\tau = 15$ s, red for $\tau = 7$ s, orange for $\tau = 10$ s, green for $\tau = 20$ s, blue for $\tau = 25$ s. The dashed line corresponds to the 99% significance level.

NoRP at 17 GHz, respectively. The spectra contain a pronounced component with a positive frequency drift during the rise and maximum phases of the flare. Five cycles of QPP are observed in a time interval of about one minute. The period of the pulsations decreases from $P \approx 17$ s in the rise phase to $P \approx 9$ s in the maximum, with a mean drift rate $\mathrm{d}P/\mathrm{d}t \approx -14\ \mathrm{s\,min^{-1}}$. The spectral analysis reveals two periods corresponding to the final and start values of the drifting component (Figure 4d). The first (left) peak on the periodogram at $P \approx 9$ s is narrow. The second (right) one looks wider. Note that the next lower frequency component is an artefact, it appears due to the main flux peak.

Two events from our list have been found to have QPPs of this type. The first one is described above. The second one occurred on 14 March 2002. During that flare, a drifting spectral component appears and evolves simultaneously with another QPP with stable period.

3.3. Pulsations with Spectral Drift to Longer Periods

The variation of the microwave emission of the flare on 03 July 2002 has an interesting spectral behaviour. According to Figure 5a, the microwave burst consists of three peaks. The first one occurs from 02:10:20 to 02:11:00 UT (from 40 – 80 s), the second one from 02:11:00 to 02:13:00 UT (80 – 240 s) and a subsequent smooth weak peak from 02:13:00 to 02:16:00 UT (240 – 420 s). Note that the source of all peaks is the same single flaring loop. Two types of pulsations are seen in the wavelet power spectrum. The first and the second peaks contain stable period QPPs (*e.g.* with a period of about 15 s and a quality $Q \approx 12$ during the decay of the first impulsive peak, see Figure 5a). This part of the burst, shown by the two vertical dashed lines in Figure 5a, is zoomed in Figure 5b for a more detailed

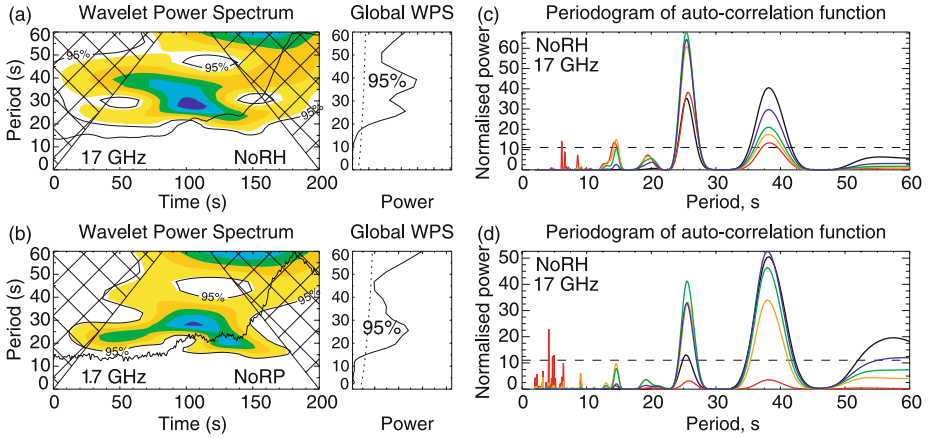

Figure 6 Analysis of the flare on 21 May 2004, 23:47:10 – 23:50:30 UT. (a) Wavelet power spectrum of the modulation signal ($\tau = 30$ s), with superimposed normalised profile of the radio emission, both obtained with NoRH at 17 GHz. The right plot is the global wavelet power spectrum. The dashed line shows the 95% significance level. (b) The same as on panel (a) but for the NoRP data. (c) Periodograms of the auto-correlation function constructed for the modulation signal obtained with NoRH at 17 GHz. (d) The same as (c) but at 34 GHz. On plots (c), (d) the black line is for $\tau = 30$ s, red for $\tau = 7$ s, orange for $\tau = 10$ s, green for $\tau = 15$ s, blue for $\tau = 20$ s; the dashed line corresponds to the 99% significance level.

view. These QPPs belong to the pulsations of the first type, discussed above and illustrated in Figure 2. Moreover, the second peak contains stable multiple periodicities, revealed by the thorough study of Inglis and Nakariakov (2009) with the application of the periodogram technique to the 17 GHz and 34 GHz signals and hard X-ray data obtained with the *Reuven Ramaty High Energy Solar Spectroscopic Imager* (RHESSI).

In the decay phase of the flare, shown in Figure 5a from the dotted line to the end, there is clear evidence of a QPP with a negative frequency drift (see Figure 5c). The period of this QPP increases from 22 s to 30 s in four to five cycles with a mean drift rate $\mathrm{d}P/\mathrm{d}t \approx 11\ \mathrm{s\,m^{-1}}$. The periodogram of the auto-correlation function of this QPP has two peaks, similar to the previous example (Figure 4d). Their values correspond to the starting and final values of the drifting component (Figure 5d).

3.4. Pulsations with an X-shaped Drift

The flare on 21 May 2004 (see Figure 6) has a peculiar QPP, which we refer to as the fourth type. Wavelet power spectra of this event show X-shaped structures drifting between the periods of 20 s and 40 s (Figure 6a, b). Two drifting spectral branches start at the beginning of the rise phase; initially, they have different periods, of about 40 s and 25 s. With time, the periods converge with a drift rate $|\mathrm{d}P/\mathrm{d}t| \approx 10\ \mathrm{s\,m^{-1}}$. In about 100 s, the branches merge into one with a period of about 30 s and then bifurcate again with a mean drift rate $|\mathrm{d}P/\mathrm{d}t| \geq 10\ \mathrm{s\,m^{-1}}$. Both branches last for about 180 s and fade away at the flare maximum. Similar wavelet spectral signatures are present in both NoRH and NoRP signals. To illustrate the reliability of the observed QPPs, here we also show results of our spectral analysis of the signal at 34 GHz. As we can see in Figure 6c and 6d, periodograms of the auto-correlation functions of the pulsations at 17 and 34 GHz both have two well-pronounced spectral peaks at periods of about 38 s and 26 s. The ratio of the periods is 0.68, indicating that these periodicities are not simple harmonics caused by a temporal non-linearity of the signal (which

would give a period ratio of 0.5). Moreover, as is evident in the wavelet spectra, the ratio changes with time from 0.68 up to one and then comes down to the initial value.

Among twelve flares under study, only one event with spectral evolution of this type was found.

4. Discussion and Conclusions

In this paper we have studied the temporal evolution of microwave QPPs from a set of twelve flares, observed simultaneously with both the *Nobeyama Radioheliograph* and the *Radio Polarimeters*. The microwave sources of all the analysed flares have a well-resolved single loop shape. The presence or absence of visible QPPs in the light curves were not taken into account in the selection of the flares for the analysis, in order to find out how common QPPs in single flaring loops are. Obviously, the applied selection criteria restrict the statistical base of our analysis. However, this approach allows us to study the variety of QPPs in a certain well-specified class of flaring events, those with a clear loop-like microwave source.

The signals were detrended and analysed using the wavelet, correlation and periodogram techniques. All the flares were processed in a similar way, resembling the approach proposed in De Moortel and McAteer (2004). It was found that in single-loop flares the presence of QPPs is quite a common phenomenon: the presence of at least one significant spectral component with a period ranging from 5 – 60 s has been found in ten out of twelve analysed events. We point out that the applied detection criterion was rather tough; only those QPPs which were confidently detected in the data of both NoRH and NoRP (*i.e.*, detected in both detrended light curves and in the auto-correlation and cross-correlation functions at 17 and 34 GHz, independent of the detrending method, and with quality greater than nine) were counted. Two events were found to have two simultaneous significant periodicities and one event had three periodicities. Two flares revealed no reliably determined periodic structures. The quality of the detected QPPs is low, with an average value of 25. The highest quality, 85, was found for the 5 s oscillation in the flare on 17 March 2003.

According to our findings, it is possible to divide phenomenologically the detected QPPs into four distinct types: *i*) those with stable mean periods in the range 5 – 20 s (eight events), *ii*) those with spectral drift to shorter periods, during the rise phase of a burst (two events), *iii*) those with drift to longer periods, during the decay phase (two events), *iv*) those with an X-shaped drift of two significant spectral components with periods of 20 – 40 s (one event). We believe that a future larger database of events may provide us with a richer set of characteristic types of microwave pulsations. We see such a possibility, for instance, from the recent observation of tadpole patterns in wavelet spectra of decimetric radio bursts (Meszarosova *et al.*, 2009).

The main result of our study is the clear evidence that the presence of an oscillatory component in flaring light curves is a widespread phenomenon, independent of the event selection criterion. This result indicates that oscillations are an intrinsic feature of flaring energy release. Thus, our understanding of solar flares cannot be complete without revealing the physical mechanisms responsible for the generation of the periodicity.

The ranges of the detected periods coincide with the expected transverse and longitudinal fast magnetoacoustic and Alfvén transit times (for Alfvén speeds in the range of several hundreds to a few thousands km s^{-1}). This suggests that the QPPs are likely to be associated with MHD oscillations in either the flaring loops or in their nearest neighbourhood. Periods P of standing fast magnetoacoustic and Alfvén modes are linked with the length L of the

oscillating structure as

$$P \approx \frac{2L}{C_{\rm ph} n}, \tag{4}$$

where n is an integer corresponding to the number of the longitudinal harmonics and $C_{\rm ph}$ is the phase speed of the mode. The value of $C_{\rm ph}$ is in the range from the Alfvén speed inside the structure, $C_{\rm Ai}$, to the external Alfvén speed, $C_{\rm Ae}$. In particular, for the torsional mode we get $C_{\rm ph} = C_{\rm Ai}$, for the long-wavelength sausage mode $C_{\rm ph} \approx C_{\rm Ae}$ and for ballooning modes $C_{\rm ph} \approx \sqrt{2} C_{\rm Ai}$ (*e.g.* Nakariakov and Melnikov, 2009). Also, the simultaneous presence of two or more periodicities in the data (multi-periodicity) found in this study supports the interpretation of the QPPs in terms of MHD oscillations. Indeed, different periods and their ratios can be easily obtained from Equation (4) if there are several different MHD modes, with different mode numbers n and phase speeds $C_{\rm ph}$, excited simultaneously in the same flaring loop. On the other hand, it does not seem to be simple to explain the multi-periodicity in terms of repetitive reconnection (see Inglis and Nakariakov, 2009 for a discussion). In the LCR-circuit model the multi-periodicity could be obtained in the case of several interacting flaring loops, which is not consistent with our observations.

The detected period modulation or drift can also be easily explained with the use of Equation (4). Indeed, the variation of the loop length, the magnetic field strength and of the plasma density caused by the evolution of the flaring structure and its neighbourhood, in response to the energy release, modifies the period of MHD oscillations. Thus, we conclude that the most likely interpretation of the periodicities detected in our study is connected with MHD oscillations. Detailed consideration of each of the twelve observations discussed above requires dedicated investigation. In particular, it would be necessary to look for any relationship between the drift of the QPP periods and the parameters of the emitting loop: its size, radio and soft X-ray brightness, the peak frequency of the gyrosynchrotron spectrum, *etc*.

We believe that our findings constitute a phenomenological basis for further progress in understanding the physical mechanisms responsible for the generation of QPPs in solar and stellar flares. A discussion of possible interpretations of the observed properties of the obtained spectral types and their detailed spatially resolved analysis is out of the scope of this paper, and will be presented in a forthcoming study.

Acknowledgements *Nobeyama Radioheliograph* is operated by Nobeyama Solar Radio Observatory/ National Astronomical Observatory of Japan. This research was partly supported by the grants of the RFBR Nos. 07-02-01066, 08-02-92228, 09-02-00624, 09-02-90448, of the Programs of RAS "Solar Activity and Physical Processes in the Sun – Earth System" and "Plasma Processes in Solar System", of the Federal Programs "Scientific and Educational Manpower of Innovative Russia" No. 02.740.11.0246, No. P683/20.05.2010, and by the Royal Society British-Russian Research Collaboration grant.

References

Andries, J., Van Doorsselaere, T., Roberts, B., Verth, G., Verwichte, E., Erdélyi, R.: 2009, *Space Sci. Rev.* **149**, 83.

Asai, A., Shimojo, M., Isobe, H., Morimoto, T., Yokoyama, T., Shibasaki, K., Nakajima, H.: 2001, *Astrophys. J.* **562**, L103.

Aschwanden, M.J.: 1987, *Solar Phys.* **111**, 113.

De Moortel, I., McAteer, R.T.J.: 2004, *Solar Phys.* **223**, 1.

Dmitriev, P.B., Kudryavtsev, I.V., Lazutkov, V.P., Matveev, G.A., Savchenko, M.I., Skorodumov, D.V., Charikov, Yu.E.: 2006, *Solar Syst. Res.* **40**, 142.

Fleishman, G.D., Bastian, T.S., Gary, D.E.: 2008, *Astrophys. J.* **684**, 1433.

Fleishman, G.D., Fu, Q.J., Huang, G.-L., Melnikov, V.F., Wang, M.: 2002, *Astron. Astrophys.* **385**, 671.
Foullon, C., Verwichte, E., Nakariakov, V.M., Fletcher, L.: 2005, *Astron. Astrophys.* **440**, L59.
Gelfreikh, G.B., Nagovitsyn, Yu.A., Nagovitsyna, E.Yu.: 2006, *Publ. Astron. Soc. Japan* **58**, 29.
Gelfreikh, G.B., Grechnev, V., Kosugi, T., Shibasaki, K.: 1999, *Solar Phys.* **185**, 177.
Grechnev, V.V., White, S.M., Kundu, M.R.: 2003, *Astrophys. J.* **588**, 1163.
Horne, J.H., Baliunas, S.L.: 1986, *Astrophys. J.* **302**, 757.
Inglis, A.R., Nakariakov, V.M.: 2009, *Astron. Astrophys.* **493**, 259.
Khodachenko, M.L., Zaitsev, V.V., Kislyakov, A.G., Stepanov, A.V.: 2009, *Space Sci. Rev.* **149**, 83.
McAteer, R.T.J., Gallagher, P.T., Bloomfield, D.S., Williams, D.R., Mathioudakis, M., Keenan, F.P.: 2004, *Astrophys. J.* **602**, 436.
Melnikov, V.F., Reznikova, V.E., Shibasaki, K., Nakariakov, V.M.: 2005, *Astron. Astrophys.* **439**, 727.
Meszarosova, H., Karlicky, M., Rybak, J., Jiricka, K.: 2009, *Astron. Astrophys.* **697**, L108.
Nakariakov, V.M., Melnikov, V.F.: 2009, *Space Sci. Rev.* **149**, 119.
Nakariakov, V.M., Melnikov, V.F., Reznikova, V.E.: 2003, *Astron. Astrophys.* **412**, L7.
Nakariakov, V.M., Foullon, C., Verwichte, E., Young, N.P.: 2006, *Astron. Astrophys.* **452**, 343.
O'Shea, E., Banerjee, D., Doyle, J.G., Fleck, B., Murtagh, F.: 2001, *Astron. Astrophys.* **368**, 1095.
Reznikova, V.E., Melnikov, V.F., Su, Y., Huang, G.: 2007, *Astron. Rep.* **51**, 588.
Shibasaki, K.: 2001, *Astrophys. J.* **550**, 1113.
Torrence, C., Compo, G.P.: 1998, *Bull. Am. Meteorol. Soc.* **79**, 61.
Zaitsev, V.V., Stepanov, A.V.: 2008, *Phys. Usp.* **51**, 1123.
Zaitsev, V.V., Stepanov, A.V., Urpo, S., Pohjolainen, S.: 1998, *Astron. Astrophys.* **337**, 887.
Zimovets, I.V., Struminsky, A.B.: 2009, *Solar Phys.* **258**, 69.